



## Effect of Flexible Chain on Mesomorphic Properties of Alkyloxy Substituted 4-Chloroazobenzene Liquid Crystals

KAMRUZZAMAN<sup>1</sup>, ROUSHOWN ALI<sup>1</sup>, RABIUL KARIM<sup>1</sup>, SAMIUL ISLAM CHOWDHURY<sup>2</sup> and TARIQUL HASAN<sup>1,\*</sup> 

<sup>1</sup>Department of Chemistry, University of Rajshahi, Rajshahi-6205, Bangladesh

<sup>2</sup>Department of Chemistry, Bangladesh University of Textile, Dhaka-1208, Bangladesh

\*Corresponding author: Fax: +880 721 750064; Tel: +880 721 711107; E-mail: [thasan.chem@ru.ac.bd](mailto:thasan.chem@ru.ac.bd)

Received: 25 January 2021;

Accepted: 29 March 2021;

Published online: 16 April 2021;

AJC-20339

Three rod-shaped alkyloxy substituted 4-chloroazobenzene liquid crystals, 1-(4-chlorophenyl)-2-[4-(alkyloxy)phenyl]diazene (hexyl, octyl and nonyl as flexible oxyalkyl chain) have been synthesized by diazotization of *p*-chloroaniline with phenol and subsequently performed etherification reaction with different alkyl bromides. The structures of the substituted 4-chloroazobenzene liquid crystals have been characterized by spectroscopic methods. The mesomorphic properties of the liquid crystals were examined by polarizing optical microscope (POM) and differential scanning calorimetry (DSC). All the oxyalkyl homologues of chloro substituted azobenzene showed enantiotropic smectic A (SmA) mesophase, which was understood clearly by the texture of the compounds employing polarizing optical microscope (POM) analysis. During heating scan in DSC analyses melting points, SmA-isotropic temperature and enthalpy changes associated with SmA-isotropic transition showed a remarkable impact on the spacer length of 4-chloro azobenzene derivatives.

**Keywords:** Liquid crystal, Azobenzene, Diazene, Mesophase, Smectic phase, Isotropic temperature.

### INTRODUCTION

The materials with liquid crystalline properties have drawn much attention to the researchers because of their wide range of potential applications in the fields of optical [1], electrical [2] and biological/medical fields [3]. Among various types of liquid crystals like calamitic (rod shaped), banana shaped and discotic liquid crystal, calamitic liquid crystal, calamitic molecules are important for their use both in academic and technological applications [4]. To utilize these materials for suitable applications, modification of the properties of liquid crystals is required and this can be done by transforming the structure as well as changing shape of the materials, such as calamitic (rod shaped) to discotic (disc-like)/banana core (bent like)/lyotropic. Another way to fit the specific liquid crystal properties [5] is to change the molecular length of various calamitic liquid crystals. Internal changes in calamitic liquid crystal can also be done by altering the polar character of the rod-like molecule [5-9]. Recently, liquid crystal system containing azobenzene mesogen unit has attracted a lot of interest as azobenzene moieties have reversible photo-isomerization process which

modify extensively the order of the mesophase [10,11]. Azobenzene derivatives are also important because of their ability of inter-changeable *cis-trans* photo-isomerization, which causes a variety of physico-chemical properties, like size, shape and polarity of the molecules [12,13]. The azobenzene-containing molecules form an anisotropic phase in *trans*-conformation, whereas, the formation of *cis*-conformation of an isotropic phase gets destroyed with ordered molecular arrangement. The azobenzene moiety with *cis-trans* photo-isomerizations have a variety of applications, such as holographic media [14,15], optical storage [16], reversible optical waveguides [17], LC photo-alignment system [18] and drug delivery [19].

The calamitic molecule consists of mesogenic core, terminal chain and lateral functional group. The core provides rigidity which is required for anisotropy while terminal chain provides flexibility to stabilize the molecular alignment. The lateral substituent of azobenzene containing molecules also play a vital role to generate mesomorphic behaviour (nematic or smectic) and properties for special applications. The polar lateral substituent depressed the smectic phase stability, whereas, lamellar packing is depended on size and polarity. With

increasing packing size and polarity of the lateral substituents, the lamellar packing is devastated. Among halogens ( $I = 1.98 \text{ \AA}$ ,  $Br = 1.80 \text{ \AA}$ ,  $Cl = 1.75 \text{ \AA}$ ,  $F = 1.47 \text{ \AA}$ ), chloro substituent makes a greater dipole than that of fluoro substituent due to longer bond to carbon but the larger size of the chloro substituent destabilizes liquid crystal phase and renders its use as lateral substituent [20]. The fluoro substituent is mostly used as halogen lateral substituent [21]. Thus, synthesis of azobenzene in the format of liquid crystal form with different lateral substituents [22,23] has drawn attention by many researchers, but still there are not enough studies with developing and designing calamitric liquid crystal particularly chlorine as a lateral substituent.

In this article, three calamitic (rod-like) low molecular weight liquid crystals composed of azobenzene as mesogen, chlorine as a lateral substituent including various alkoxy as flexible chain are synthesized and characterized. Finally, the mesomorphism properties of the synthesized crystals have been compared.

## EXPERIMENTAL

*p*-Chloro aniline was purchased from Loba Chemie Pvt. Ltd., India. Sodium nitrite was purchased from Thomas-Baker (chemicals) Ltd., India. 1-Bromo hexane, 1-bromo octane and 1-bromo nonane were procured from Fluka Chemicals Ltd. All solvents used in this work were purified over distillation followed by refluxed with sodium.

**Characterization:** The structures of the synthesized compounds were confirmed by the spectroscopic analyses.  $^1\text{H}$  NMR analyses were carried out with BRUKER spectrometer operated at 400 MHz in pulse Fourier transform mode and chloroform- $d_6$  was used as solvent. IR spectra were recorded with KBr using Perkin-Elmer spectrum-100 FT-IR spectrometer. UV-visible spectra were obtained by using Shimadzu UV-1650PC spectrometer. The enthalpies of transitions (reported in  $\text{J g}^{-1}$ ) and phase transition temperature were determined by using Perkin-Elmer DSC-8000. Both the heating and cooling rate in DSC were  $10 \text{ }^\circ\text{C}/\text{min}$ . The textures of the phase transition of the compounds were obtained using Olympus BX53 hot-stage polarizing optical microscope.

**Synthetic procedure of 4-[(4-chlorophenyl)diazinyl]phenol (CDP):** The synthesis of CDP was carried out by following similar procedure reported earlier [24,25]. In an ice bath, a mixture of 100 mL PEG400/1,4-dioxane/water (60/30/10) was cooled and to this mixture, 6.75 mL (78.4 mmol) of concentrated HCl and 5 g (39.2 mmol) of *p*-chloroaniline were added. To this mixture, a solution of 10 mL  $\text{NaNO}_2$  (2.98 g, 43.1 mmol) was added dropwise for the formation of diazo-

nium salt. The mixture was stirred continuously for 2 h in the temperature range  $0$  to  $5 \text{ }^\circ\text{C}$ . A 100 mL solution was prepared with phenol (11.07 g, 117.6 mmol), NaOH (1.72g, 43.1 mmol) and mixed solvent PEG400/1,4-dioxane/water (60/30/10) in another flask and then poured into the above mixture (diazonium salt). The solution was stirred for further 0.5 h and 200 mL water was added. The solution was made acidic ( $\text{pH} = 5$ ) by adding about 2.5 mL of HCl. The product was obtained as red powder, filtered off, washed several times with water and dried by vacuum. The crude product was purified by chromatography (silica gel) using petroleum ether:acetone (95:5) as eluent. Finally, a red powder product (yield 5.9 g, 65%) was obtained (**Scheme-I**).

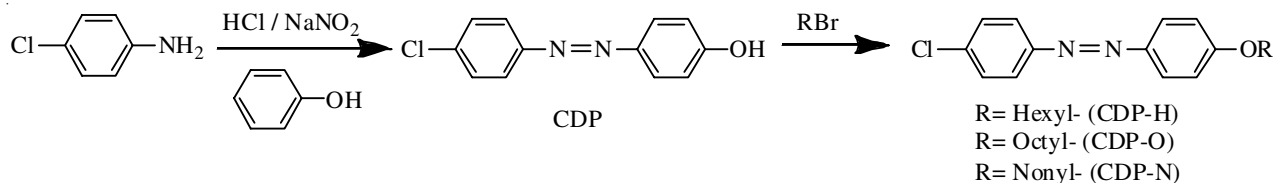
**4-[(4-Chlorophenyl)diazinyl]phenol (CDP):** Red powder, yield: 65%,  $R_f$  value 0.43 in petroleum ether:acetone (9:4).  $^1\text{H}$  NMR ( $\text{CDCl}_3$ ),  $\delta$  ppm: 6.94 (2H, d), 7.46 (2H, d), 7.83 (2H, d), 7.88 (2H, d), 5.27 (1H, s, Ar-OH).  $^{13}\text{C}$  NMR ( $\text{CDCl}_3$ ),  $\delta_c$  ppm: 116, 124, 125, 129, 136, 147, 151, 158. IR (KBr,  $\nu_{\text{max}}$ ,  $\text{cm}^{-1}$ ): 3413, 1638, 1617, 1589, 1576, 1477, 1225, 1082, 838, 724.

**Synthesis of alkoxy derivatives of CDP (CDP-H, CDP-O and CDP-N):** All the alkoxy derivatives of CDP were synthesized following the procedure [26] as described below:

A mixture of 0.2 g (0.86 mmol) of CDP and 0.48 g (3.45 mmol) of  $\text{K}_2\text{CO}_3$  was added in 20 mL of dry acetone in a 250 mL round bottomed flask and stirred for 0.5 h. Then, 1.72 mmol of 1-bromo alkane (1-bromo hexane/1-bromo octane/1-bromo nonane) was added to the mixture and the reaction mixture was refluxed in an oil bath at  $65 \text{ }^\circ\text{C}$  for 24 h. The reaction progress was checked by thin layer chromatography (TLC). When the reaction was completed, the mixture was allowed to cool. The residue obtained was filtered off and the filtrate was concentrated in vacuum. The solid product thus obtained was dissolved in 25 mL of ether and the solution was washed with water, 10% NaOH and again water for three times. Finally, the ether solution was dried over  $\text{MgSO}_4$ . The solution was then concentrated in vacuum and the crude product was purified by recrystallization in petroleum ether. In each case, the pure product was obtained as orange crystal.

**1-(4-Chlorophenyl)-2-[4-(hexyloxy)phenyl]diazene (CDP-H):** Orange micro crystal, yield 0.2 g (75%),  $R_f$  value 0.90 in petroleum ether:acetone (9:2).  $^1\text{H}$  NMR ( $\text{CDCl}_3$ ),  $\delta$  ppm: 7.88 (2H, d), 7.81 (2H, d), 7.46 (2H, d), 6.98 (2H, d), 4.03 (2H, t), 1.81 (2H, m), 1.48 (2H, m), 1.34 (4H, m), 0.92 (3H, t).  $^{13}\text{C}$  NMR ( $\text{CDCl}_3$ ),  $\delta_c$ , ppm: 14, 23, 26, 29, 32, 68, 115, 124, 125, 129, 136, 147, 151, 162. IR (KBr,  $\text{cm}^{-1}$ ): 2949, 2866, 1637, 1617, 1584, 1501, 1417, 1260, 1138, 1084, 844, 724. UV ( $\lambda_{\text{max}}$ ): 252 nm ( $\sigma \rightarrow \sigma^*$ ), 356 nm ( $\pi \rightarrow \pi^*$ ), 448 nm ( $n \rightarrow \pi^*$ ).

**1-(4-Chlorophenyl)-2-[4-(octyloxy)phenyl]diazene (CDP-O):** Orange needle shaped crystal, yield 0.23 g (76%),



**Scheme-I:** Synthetic route of 4-chloroazobenzene derivatives

$R_f$  value 0.91 in petroleum ether:acetone (9:2).  $^1\text{H NMR}$  ( $\text{CDCl}_3$ ),  $\delta$  ppm: 7.89 (2H, d), 7.83 (2H, d), 7.46 (2H, d), 7.01 (2H, d), 4.04 (2H, t), 1.82 (2H, m), 1.49 (2H, m), 1.36 (8H, m), 0.92 (3H, t).  $^{13}\text{C NMR}$  ( $\text{CDCl}_3$ ),  $\delta_c$  ppm: 14, 23, 26, 29, 29, 29, 32, 68, 115, 124, 125, 129, 136, 147, 151 and 162. IR (KBr,  $\text{cm}^{-1}$ ): 2927, 2851, 1638, 1584, 1500, 1470, 1416, 1256, 1138, 1087, 844, 725. UV ( $\lambda_{\text{max}}$ ): 251 nm ( $\sigma \rightarrow \sigma^*$ ), 356 nm ( $\pi \rightarrow \pi^*$ ), 439 nm ( $n \rightarrow \pi^*$ ).

**1-(4-Chlorophenyl)-2-[4-(nonyloxy)phenyl]diazene, (CDP-N):** Orange micro crystal, yield 0.24 g (78%),  $R_f$  value 0.94 in petroleum ether:acetone (9:2).  $^1\text{H NMR}$  ( $\text{CDCl}_3$ ),  $\delta$  ppm: 7.89 (2H, d), 7.83 (2H, d), 7.46 (2H, d), 7.01 (2H, d), 4.04 (2H, t), 1.82 (2H, m), 1.48 (2H, m), 1.30 (10H, m), 0.89 (3H, t).  $^{13}\text{C NMR}$  ( $\text{CDCl}_3$ ),  $\delta_c$  ppm: 14, 23, 26, 29, 29, 29, 30, 32, 68, 115, 124, 125, 129, 136, 147, 151 and 162. IR (KBr,  $\text{cm}^{-1}$ ): 2951, 2937, 2919, 2849, 1638, 1617, 1603, 1584, 1502, 1472, 1256, 1144, 1090, 845, 728. UV ( $\lambda_{\text{max}}$ ): 252 nm ( $\sigma \rightarrow \sigma^*$ ), 357 nm ( $\pi \rightarrow \pi^*$ ), 440 nm ( $n \rightarrow \pi^*$ ).

## RESULTS AND DISCUSSION

4-[(4-Chlorophenyl)diazinyl]phenol (CDP) was synthesized by diazotization reaction between *p*-chloroaniline and phenol (**Scheme-I**). The pure CDP was obtained as red powder separated by column chromatographic technique.

In  $^1\text{H NMR}$  spectrum of CDP (Fig. 1a), signals at 6.94–7.88 ppm were assigned for aromatic protons and a singlet at 5.27 was appeared for Ar-OH proton. In  $^{13}\text{C NMR}$  spectrum of CDP (Fig. 2a), four peaks observed at 116–129 ppm were assigned to be eight carbons of aromatic ring and signals at 136 and 147 ppm were assigned for HO-C and Cl-C, respectively. The signals appeared at 151 and 158 ppm were assigned for two carbons adjacent to azo group. In IR spectrum, absorption peaks at 3413 and 1589  $\text{cm}^{-1}$  were appeared for –OH and azo groups, respectively. The above spectroscopic data confirmed the structure of CDP.

The CDP was used as a precursor for synthesizing different oxyalkyl (hexyl, octyl and nonyl) containing azobenzene derivatives *i.e.* 1-(4-chlorophenyl)-2-[4-(hexyloxy)phenyl]diazene (CDP-H), 1-(4-chlorophenyl)-2-[4-(octyloxy)phenyl]diazene (CDP-O) and 1-(4-chlorophenyl)-2-[4-(nonyloxy)phenyl]diazene (CDP-N) by alkylation with corresponding alkyl bromide as described in the experimental section.

In  $^1\text{H NMR}$  spectrum of CDP-H (Fig. 1b), the signals at 6.98–7.88 ppm were assigned for aromatic protons and a triplet at 4.03 ppm was appeared for the –OCH<sub>2</sub> protons. The peaks at 1.81 (2H, m), 1.48 (2H, m), 1.34 (4H, m) and 0.92 (3H, t) ppm were appeared for the eleven aliphatic protons of hexyl group. In  $^{13}\text{C NMR}$  spectrum of CDP-H (Fig. 2b), four peaks at 115–129 ppm were assigned for the eight carbons of aromatic ring and five peaks observed at 14–32 ppm were assigned for five carbons of the hexyl group. The peak at 68 ppm was assigned for the carbon of –OCH<sub>2</sub> group. The peaks observed at 136 and 147 ppm were assigned for HO-C and Cl-C, respectively. The peaks at 151 and 162 ppm were attributed for two carbons adjacent to azo group. In IR spectrum, absorption peaks at 2949–2866  $\text{cm}^{-1}$  were appeared for C-H stretching vibration and the signal at 1584  $\text{cm}^{-1}$  was assigned for azo group. In the

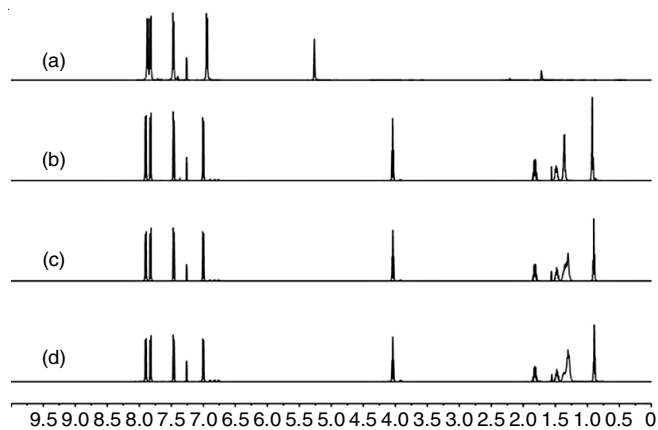


Fig. 1.  $^1\text{H NMR}$  spectra of (a) CDP, (b) CDP-H, (c) CDP-O and (d) CDP-N

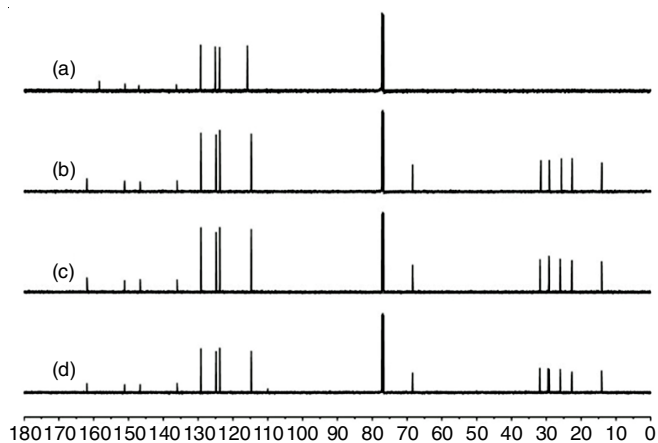


Fig. 2.  $^{13}\text{C NMR}$  spectra of (a) CDP, (b) CDP-H, (c) CDP-O and (d) CDP-N

UV spectrum, a  $\pi \rightarrow \pi^*$  transition was observed at 357 nm which indicated the presence of azo group.

In  $^1\text{H NMR}$  spectrum of CDP-O (Fig. 1c), the peaks at 7.01–7.89 and a triplet at 4.04 ppm were assigned for aromatic and –OCH<sub>2</sub> protons, respectively. The peaks at 1.82 (2H, m), 1.49 (2H, m), 1.36 (8H, m) and 0.92 (3H, t) ppm were appeared for the fifteen aliphatic protons of octyl group. In  $^{13}\text{C NMR}$  spectrum of CDP-O (Fig. 2c), four peaks observed at 115–129 ppm were assigned for eight carbons of aromatic ring and the peaks observed at 14–32 ppm were appeared for seven carbons of octyl group. The peaks at around 68 ppm were assigned for the carbon of –OCH<sub>2</sub> group. The peaks at 136 and 147 ppm were assigned for HO-C and Cl-C, respectively. The peaks at 151 and 162 ppm were appeared for two carbons adjacent to azo group. In IR spectrum, absorption peaks at 2927–2851  $\text{cm}^{-1}$  were appeared for C-H stretching vibration and the signal at 1584  $\text{cm}^{-1}$  was assigned for azo group. In UV spectrum, a  $\pi \rightarrow \pi^*$  transition was observed at 356 nm, which indicated the presence of azo group.

In  $^1\text{H NMR}$  spectrum of CDP-N (Fig. 1d), the peaks at 7.01–7.89 ppm were assigned for aromatic protons and a triplet at 4.04 ppm was appeared for the –OCH<sub>2</sub> protons. The peaks at 1.82 (2H, m), 1.48 (2H, m), 1.30 (10H, m) and 0.89 ppm (3H, t) were appeared for the seventeen aliphatic protons of nonyl group. In  $^{13}\text{C NMR}$  spectrum of CDP-N (Fig. 2d), the peaks at 115–129 ppm were assigned for eight carbons of

aromatic ring and the peaks at 14-32 ppm were appeared for eight carbons of nonyl group. The peaks at 68 ppm were assigned for the carbon of  $-OCH_2$  group. The peaks at 136 and 147 ppm were assigned for HO-C and Cl-C, respectively. The peaks at 151 and 162 ppm were appeared for two carbons adjacent to azo group. In IR spectrum, absorption peak at 2951-2849  $cm^{-1}$  were appeared for C-H stretching vibration and the signal at 1584  $cm^{-1}$  was assigned for azo group. In UV spectrum, a  $\pi \rightarrow \pi^*$  transition was observed at 357 nm which indicated the presence of azo group.

**Mesomorphic behaviour:** The mesomorphic behaviour of the compounds were analyzed by differential scanning calorimetry (DSC) and optical polarizing microscope (POM). The phase transition temperature associated with transition enthalpies were determined by DSC with 2<sup>nd</sup> heating and 1<sup>st</sup> cooling scans and are summarized in Table-1. The DSC curves of the compounds CDP-H, CDP-O and CDP-N are presented in Fig. 3. Two transitions observed in both heating and cooling scan as a result of enantiotropic phase transition present in the curve of all these compounds. On heating scan, the Cr-SmA and SmA-I transitions were observed at 87.66 and 93.26 °C for CDP-H, 82.08 and 97.39 °C for CDP-O and 91.29 and 96.82 °C for CDP-N, respectively. The DSC data revealed that the melting point of CDP-H and CDP-O (even carbon containing flexible chain) were decreased with increasing of alkyl chain, hence mesophase stability was increased. But the melting point of CDP-N (odd carbon containing flexible chain) was increased although the length of alkyl chain was increased, which differed from the theoretical manner, hence mesophase stability was decreased in heating scan, keeping in view of this behaviour to show hypothetical probable odd-even effect [27-29].

On cooling scan, the I-SmA and SmA-Cr transitions were observed at 89.98 and 62.54 °C for CDP-H, 95.34 and 63.22 °C for CDP-O and 93.81 and 60.15 °C for CDP-N, respectively.

There was no such alteration found in cooling scan like heating scan as the mesophase stability was increased with the increasing the length of alkyl chain.

The phase textures of compounds CDP-H, CDP-O and CDP-N were investigated by using polarizing optical microscope (POM) with hot stage for identification of mesomorphic phase. All compounds were stable during repeated heating and cooling. DSC and POM data were showed a good agreement with each other. The phase textures of CDP-H, CDP-O and CDP-N are displayed in Fig. 4. Texture of all homologues were purely smectogenic, smectic A (SmA) mesophase was appeared during heating and cooling and characterized by battonetes formation on cooling and focal conic fan shaped structure. These results suggested that dipole moment and polarity of CDP-H, CDP-O and CDP-N were similar and irrespective to the length of alkyloxy groups.

When these three compounds were heated up, focal conic fan shaped texture was observed (Fig. 4a,c,e) and on further cooling, the formation of battonetes (Fig. 4b,d) that link up to form focal conic fan shaped (Fig. 4f) texture of SmA was observed. The three compounds were obtained as very stable crystal form at room temperature.

## Conclusion

In this work, three rod-shaped alkyloxy substituted 4-chloroazobenzene liquid crystals with low molecular weight were synthesized and the structure of the products were confirmed by spectroscopic analyses. Chlorine was used as a lateral substituent and various oxyalkyl as flexible unit (hexyl, octyl and nonyl). Each homologue of chloro substituted azobenzene showed enantiotropic Smectic A (SmA) liquid crystal in both heating and cooling scans. Hexyl and octyl derivative of chloro substituted azobenzene showed more stable SmA phase than that of nonyl derivative.

TABLE-1  
RESULT OBTAINED FROM DSC STUDIES

| Compounds | Transition temperature (°C) association with transition enthalpy (J/g) |   |
|-----------|--|---|
|           | 2 <sup>nd</sup> Heating  | 1 <sup>st</sup> Cooling                                   |
| CDP-H     | Crystal 87.66 (90.21), Smectic A 93.26 (8.51), Isotropic               | Isotropic 89.98 (15.72), Smectic A 62.54 (83.68), Crystal |
| CDP-O     | Crystal 82.08 (106.38), Smectic A 97.39 (18.31), Isotropic             | Isotropic 95.34 (18.65), Smectic A 63.22 (96.91), Crystal |
| CDP-N     | Crystal 91.29 (110.70), Smectic A 96.82 (13.47), Isotropic             | Isotropic 93.81 (18.39), Smectic A 60.15 (92.14), Crystal |

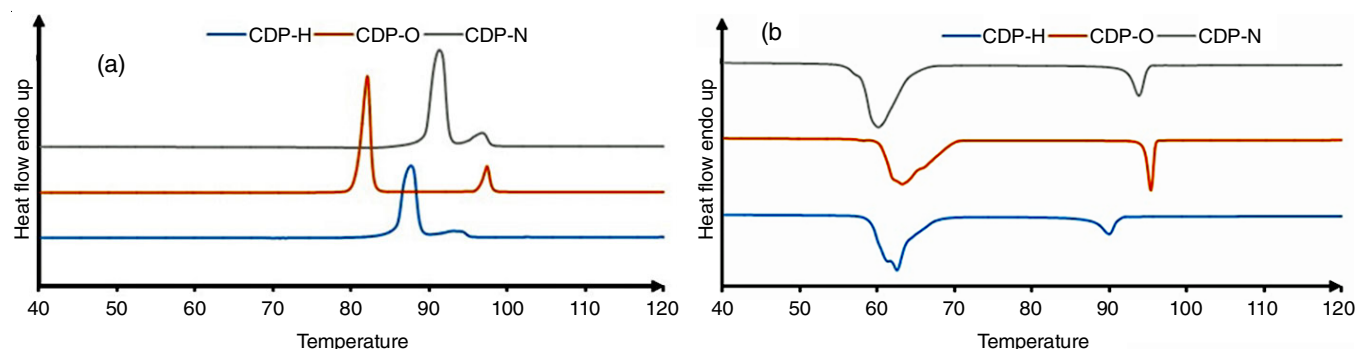


Fig. 3. DSC curve of the compounds CDP-H, CDP-O and CDP-N, (a) 2<sup>nd</sup> heating and (b) 1<sup>st</sup> cooling (temperature increasing/decreasing rate 10 °C/min)



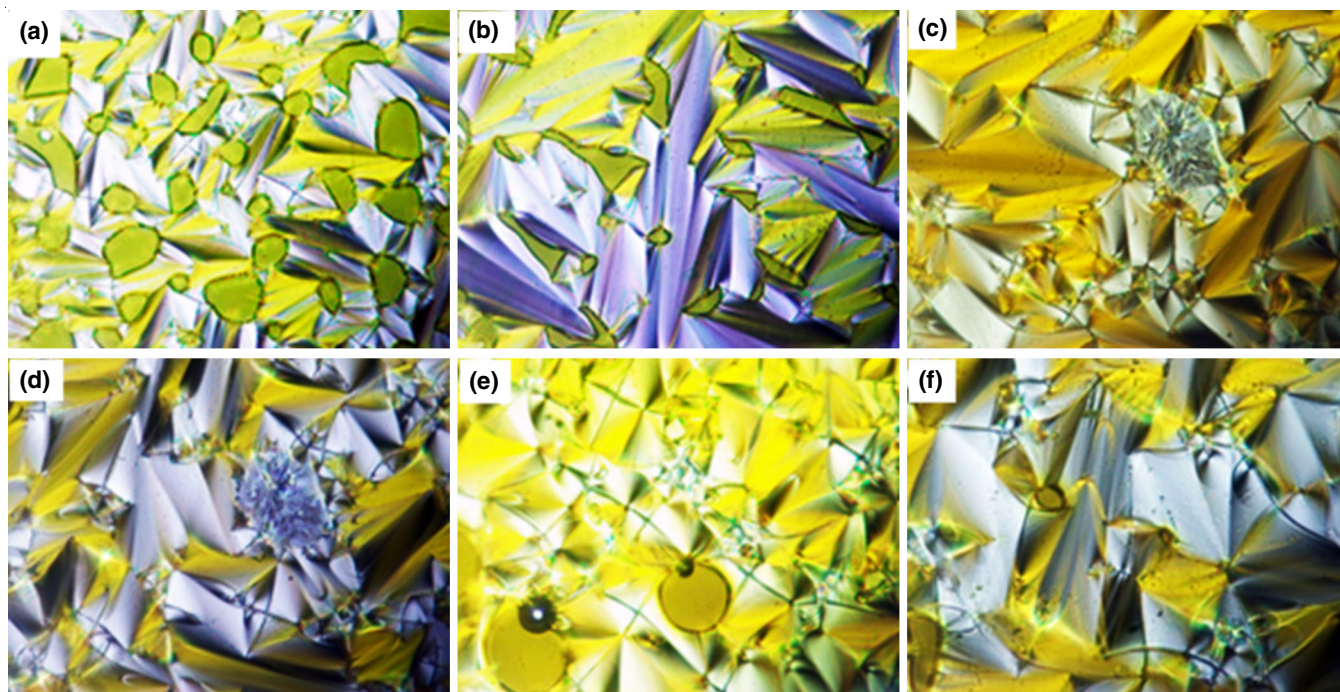


Fig. 4. Polarizing optical microscope textures (a) smectic A phase on heating to isotropic liquid of CDP-H, (b) smectic A phase on cooling from isotropic liquid of CDP-H, (c) smectic A phase on heating to isotropic liquid of CDP-O, (d) smectic A phase on cooling from isotropic liquid of CDP-O, (e) smectic A phase on heating to isotropic liquid of CDP-N and (f) smectic A phase on cooling from isotropic liquid of CDP-N (cross polarizer magnification  $\times 50$ ).

#### ACKNOWLEDGEMENTS

The authors thankfully acknowledge the support of Wazed Miah Science Research Centre, Jahangirnagar University, Savar, Bangladesh for recording  $^1\text{H}$  &  $^{13}\text{C}$  NMR and Central Science Laboratory, University of Rajshahi, Rajshahi, Bangladesh for recording IR, UV, polarizing optical microscope (POM) and differential scanning calorimetry (DSC). This work was supported by the Ministry of Science and Technology, Bangladesh through special allocation for Science and Technology [Grant No. 39.00.0000.09.02.90.18-09/922 (SL, No.528, Gr. SL. No.7 PHYS)].

#### CONFLICT OF INTEREST

The authors declare that there is no conflict of interests regarding the publication of this article.

#### REFERENCES

- V.P. Shibaev and A.Yu. Bobrovsky, *Russian Chem. Rev.*, **86**, 1024 (2017); <https://doi.org/10.1070/RCR4747>
- J. Yan, J. Lin, Q. Li and R.-Z. Li, *J. Appl. Phys.*, **125**, 024501 (2019); <https://doi.org/10.1063/1.5081766>
- S.J. Woltman, G.D. Jay and G.P. Crawford, *Nature Mater.*, **6**, 929 (2007); <https://doi.org/10.1038/nmat2010>
- S.A. Hudson and P.M. Maitlis, *Chem. Rev.*, **93**, 861 (1993); <https://doi.org/10.1021/cr00019a002>
- N. Kapernaum, F. Knecht, C.S. Hartley, J.C. Roberts, R.P. Lemieux and F. Giesselmann, *Beilstein J. Org. Chem.*, **8**, 1118 (2012); <https://doi.org/10.3762/bjoc.8.124>
- J. Romiszewski, P.T. Zita, J. Mieczkowski and E. Gorecka, *New J. Chem.*, **38**, 2927 (2014); <https://doi.org/10.1039/C4NJ00298A>
- A. Tavares, O.M.S. Ritter, U.B. Vasconcelos, B.C. Arruda, A. Schrader, P.H. Schneider and A.A. Merlo, *Liq. Cryst.*, **37**, 159 (2010); <https://doi.org/10.1080/02678290903432098>
- D.S. Rampon, F.S. Rodembusch, P.F.B. Gonçalves, R.V. Lourega, A.A. Merlo and P.H. Schneider, *J. Braz. Chem. Soc.*, **21**, 2100 (2010); <https://doi.org/10.1590/S0103-50532010001100011>
- D.J. Timmons, A.J. Jordan, A.A. Kirchon, N.S. Murthy, T.J. Siemers, D.P. Harrison and C. Slebodick, *Liq. Cryst.*, **44**, 1436 (2017); <https://doi.org/10.1080/02678292.2017.1281450>
- Y. Zhu and X. Wang, *Polym. Chem.*, **4**, 5108 (2013); <https://doi.org/10.1039/c3py00757j>
- A. Natansohn and P. Rochon, *Chem. Rev.*, **102**, 4139 (2002); <https://doi.org/10.1021/cr970155y>
- H. Rau, Eds.: J.F. Rabeck, Photochemistry and Photophysics, Boca Raton: CRC Press, vol. 11, p. 119 (1990).
- S. Hernandez-Ainsa, R. Alcalá, J. Barbera, M. Marcos, C. Sanchez and J.L. Serrano, *Eur. Polym. J.*, **47**, 311 (2011); <https://doi.org/10.1016/j.eurpolymj.2010.11.013>
- P. Rochon, E. Batalla and A. Natanson, *Appl. Phys. Lett.*, **66**, 136 (1995); <https://doi.org/10.1063/1.113541>
- D.Y. Kim, S.K. Tripathy, L. Li and J. Kumar, *J. Appl. Phys. Lett.*, **66**, 1166 (1995); <https://doi.org/10.1063/1.113845>
- H.A. Haus, *J. Opt. Soc. Am. B*, **18**, 1777 (2001); <https://doi.org/10.1364/JOSAB.18.001777>
- M.S. Ho, A. Natansohn, C. Barrett and P. Rochon, *Can. J. Chem.*, **73**, 1773 (1995); <https://doi.org/10.1139/v95-218>
- K. Ichimura, *Chem. Rev.*, **100**, 1847 (2000); <https://doi.org/10.1021/cr980079e>
- T. Yamaoka, Y. Makita, H. Sasatani, S.I. Kim and Y. Kimura, *J. Control. Rel.*, **66**, 187 (2000); [https://doi.org/10.1016/S0168-3659\(99\)00270-9](https://doi.org/10.1016/S0168-3659(99)00270-9)
- P.J. Collings and H. Michael, Introduction to Liquid Crystals Chemistry and Physics, London, UK, Taylor & Francis Ltd., edn 1 (1997).
- G. Hegde, G. Shanker, S.M. Gan, A.R. Yuvaraj, S. Mahmood and U.K. Mandal, *Liq. Cryst.*, **43**, 1578 (2016); <https://doi.org/10.1080/02678292.2016.1189001>

22. K. Krohn, M. John and E.I. Demikhov, *Russ. Chem. Bull. (Int. Ed.)*, **50**, 1248 (2001);  
<https://doi.org/10.1023/A:1014062924656>
23. S. Hernandez-Ainsa, R. Alcal, J. Barbera, M. Marcos, C. Sanchez and J.L. Serrano, *Macromolecules*, **43**, 2660 (2010);  
<https://doi.org/10.1021/ma902766j>
24. M.H. Li, P. Auroy and P. Keller, *Liq. Cryst.*, **27**, 1497 (2000);  
<https://doi.org/10.1080/026782900750018663>
25. M. Wang, L.X. Guo, B.P. Lin, X.Q. Zhang, Y. Sun and H. Yang, *Liq. Cryst.*, **43**, 1626 (2016);  
<https://doi.org/10.1080/02678292.2016.1191686>
26. Organic Syntheses Collection, vol. 3, p.140 (1955); vol. 25, p. 9 (1945).
27. T. Itahara and H. Tamura, *Mol. Cryst. Liq. Cryst.*, **501**, 94 (2009);  
<https://doi.org/10.1080/15421400802697665>
28. S.A.A. Sanches, W.C. Costa, I.H. Bechtold, R.A.P. Halfen, A.A. Merlo and L.F. Campo, *Liq. Cryst.*, **46**, 655 (2019);  
<https://doi.org/10.1080/02678292.2018.1517226>
29. W.K. Lee, K.N. Kim, F.A. Achard and J.I. Jin, *J. Mater. Chem.*, **16**, 2289 (2006);  
<https://doi.org/10.1039/b516141j>